

Development of a Highly Specialized cDNA Array for the Study and Diagnosis of Epithelial Ovarian Cancer

G. Peter Sawiris, Cheryl A. Sherman-Baust, Kevin G. Becker, Chris Cheadle, Diane Teichberg, and Patrice J. Morin¹

Laboratory of Cellular and Molecular Biology [G. P. S., C. A. S-B., P. J. M.] and DNA Array Unit [K. G. B., C. C., D. T.], Gerontology Research Center, National Institute on Aging, Baltimore Maryland 21224

ABSTRACT

Ovarian cancer is a major cause of cancer death in women. Unfortunately, the molecular pathways underlying ovarian cancer progression are poorly understood, making the development of novel diagnostic and therapeutic strategies difficult. On the basis of our previous observations obtained from serial analysis of gene expression, we have constructed a specialized cDNA array for the study of ovarian cancer. Small, specialized arrays have several practical advantages and can reveal information that is lost in the “noise” generated by irrelevant genes present in larger arrays. The array, which we named Ovachip, contains 516 cDNAs chosen from our serial analysis of gene expression and cDNA array studies for their relevance to ovarian cancer. The gene expression patterns revealed with the Ovachip are highly reproducible and extremely consistent among the different ovarian specimens tested. This array was extremely sensitive at differentiating ovarian cancer from colon cancer based on expression profiles. The Ovachip revealed clusters of coordinately expressed genes in ovarian cancer. One such cluster, the IGF2 cluster, is particularly striking and includes the insulin-like growth factor II, the cisplatin resistance-associated protein, the checkpoint suppressor 1, the cyclin-dependent kinase 6, and a protein tyrosine phosphatase receptor. We also identified a cluster of down-regulated genes that included the cyclin-dependent kinase 7 and cyclin H. Thus, the Ovachip allowed us to identify previously unidentified clusters of differentially expressed genes that may provide new paradigms for molecular pathways important in ovarian malignancies. Because of the relevance of the arrayed genes, the Ovachip may become a powerful tool for investigators in the field of ovarian cancer and may facilitate progress in understanding the etiology of this disease and in its clinical management.

INTRODUCTION

EOC² is the most lethal of gynecological malignancies in the United States and other westernized countries. This is because of difficulties of early diagnosis (1) and frequent resistance of these tumors to chemotherapy (2). In fact, a majority of EOC patients eventually die with drug-resistant cancers. Unfortunately, the specific molecular pathways important for the development of this disease have remained elusive. Alterations in *p53*, *K-Ras*, *HER-2/neu*, *c-Myc*, and many other genes have been reported in ovarian cancer, but the prevalence of these alterations depends greatly on the cohort and subtype, and do not represent ovarian-specific alterations (3, 4). Gains and losses of various chromosomal regions are common in EOC (5), but the target genes have remained elusive.

Recently, gene expression profiling techniques have provided many insights into the complexity of gene regulation in ovarian cancer.

Studies with large cDNA arrays have identified many differentially expressed genes, some of which may become useful EOC biomarkers (6–8). In addition, we have used SAGE to investigate gene expression in EOC (9). This study led to the identification of many differentially expressed genes. Notably, several of the genes identified by SAGE such as *MUC1*, the FR, and CA-125 (identified as an expressed sequence tag in our study) were known to be elevated in EOC. Others were implicated in this disease for the first time. These genes included claudin-3 and claudin-4, SLPI, and many more. Many of the genes identified as up-regulated by SAGE appeared coordinately regulated in EOC, suggesting the presence of few pathways crucial for ovarian tumorigenesis (10).

Although many of the genes identified by SAGE as highly and consistently elevated were confirmed by real-time RT-PCR (10), many more genes remained unconfirmed, and their role in EOC remained unclear. To allow for the study of the genes that are most relevant to ovarian tumorigenesis, we have built a specialized cDNA array consisting of 516 genes chosen based on our SAGE and other cDNA array data. One of the advantages of specialized arrays is that they do not include irrelevant genes that may contribute to noise during the data analysis (11). The Ovachip may be useful to many investigators interested in various aspects of ovarian cancer such as diagnosis, therapy, and drug resistance.

MATERIALS AND METHODS

Tumors Specimens and Cell Lines. The ovarian tumors were obtained from the Collaborative Human Tissue Network, Gynecological Oncology Group (Children’s Hospital, Columbus, OH). All of the ovarian specimens were diagnosed as stage III or stage IV papillary serous adenocarcinoma. Colorectal carcinoma specimens (stage T3) were a gift of Dr. Bert Vogelstein (Howard Hughes Medical Institute, Baltimore, MD). Cell lines used in this study have been described elsewhere (9). IOSE29EC was generously provided by Dr. Nelly Auersperg (University of British Columbia, Vancouver, British Columbia, Canada; Ref. 12).

Construction of a Specialized Ovarian cDNA Microarray. The selection of genes for the specialized ovarian array (the Ovachip) was made using two datasets. First, genes up-regulated or down-regulated in ovarian cancer were chosen based on our SAGE data (9). Genes that exhibited at least 5-fold up-regulation or down-regulation in at least one ovarian tumor were included. In addition, a preliminary analysis with a 15,000-gene array revealed many genes differentially expressed in ovarian cancer. The most highly differentially expressed genes identified with this array were also included on the Ovachip. A total of 516 cDNA clones were selected for constructing the Ovachip, and the entire list of genes is available online.³ The expressed sequence tag clones were obtained from Research Genetics (Huntsville, AL). After amplification, the PCR products were analyzed by agarose gel electrophoresis to determine the quality and specificity of the PCR products. In addition, over 300 of the cDNA clones were sequenced to confirm their identity and their positions on the array. PCR products were denatured and spotted in triplicate onto nylon membrane (Schleicher & Schull, Keene, NH) using a GMS 417 Arrayer (Affymetrix, Santa Clara, CA). Although a nylon membrane was used for these experiments, the reference set of cDNAs can in principle be used with a variety of platforms. Indeed, we are currently investigating the use glass slides for Ovachip construction. For sample analysis using the Ovachip, total RNA from

Received 12/21/01; accepted 2/26/02.

The costs of publication of this article were defrayed in part by the payment of page charges. This article must therefore be hereby marked *advertisement* in accordance with 18 U.S.C. Section 1734 solely to indicate this fact.

¹ To whom requests for reprints should be addressed, at Laboratory of Cellular and Molecular Biology, Gerontology Research Center, National Institute on Aging, NIH, 5600 Nathan Shock Drive, Baltimore MD 21224. Email: morinp@grc.nia.nih.gov.

² The abbreviations used are: EOC, epithelial ovarian cancer; SAGE, serial analysis of gene expression; FR, folate receptor; RT-PCR, reverse transcription-PCR; P_{ov}, Ovachip Pearson Correlation Coefficient; MDS, multidimensional scaling; TAL-1, T-cell acute lymphocytic leukemia; TCEB1, transcription elongation factor B III; PMSA1, proteasome macropain β subunit; ApoE, apolipoprotein E; CRA, cisplatin resistance-associated protein; LOI, loss of imprinting; CAK, cyclin activated kinase; cdk, cyclin-dependent kinase.

³ Internet address: <http://www.grc.nia.nih.gov/branches/lbc/ovachip.htm>.

the various tissues was isolated from guanidium isothiocyanate cell lysates by centrifugation on CsCl (9). cDNA synthesis, probe preparation, and hybridizations to the array were done essentially as described (13).

Real Time RT-PCR. Total RNA (1 μ g) from selected ovarian and colon samples was used to generate cDNA using the Taqman Reverse Transcription Reagents (PE Applied Biosystems, Foster City, CA). Similarly, cDNA was prepared using RNA from OVT6, OVT8, and IOSE29EC, and included as control. The SYBR Green I assay and the GeneAmp 5700 Sequence Detection System (PE Applied Biosystems) were used for detecting real-time PCR products as described previously (9). Primers for four candidate genes (TAL-1, EFB, PSMA1 β subunit, and ApoE) and glyceraldehyde-3-phosphate dehydrogenase as control were designed to cross intron-exon boundaries to distinguish PCR products generated from genomic *versus* cDNA template. The primer sequences are available from the authors on request.

Computational Analyses. Results from three independent hybridizations were obtained for each probe and analyzed by Array-Pr Analyzer software version 4.0 (Media Cybernetics, L.P., Des Moines, IA). Expression data for all of the specimens were compared with the nonmalignant sample IOSE29EC as reference. After normalization, the signal intensity values were fed into the Cluster program (Version 3.1), which arranged the genes hierarchically using complete linkage clustering, and then visualized with Treeview Version 1.6.6 (14). Biological expression patterns of the differentially expressed genes were processed for presentation using GeneSpring software (version 4.0.7; Silicon Genetics, San Carlos, CA). All of the MDS analyses were performed using BRB ArrayTools developed previously (15).

RESULTS

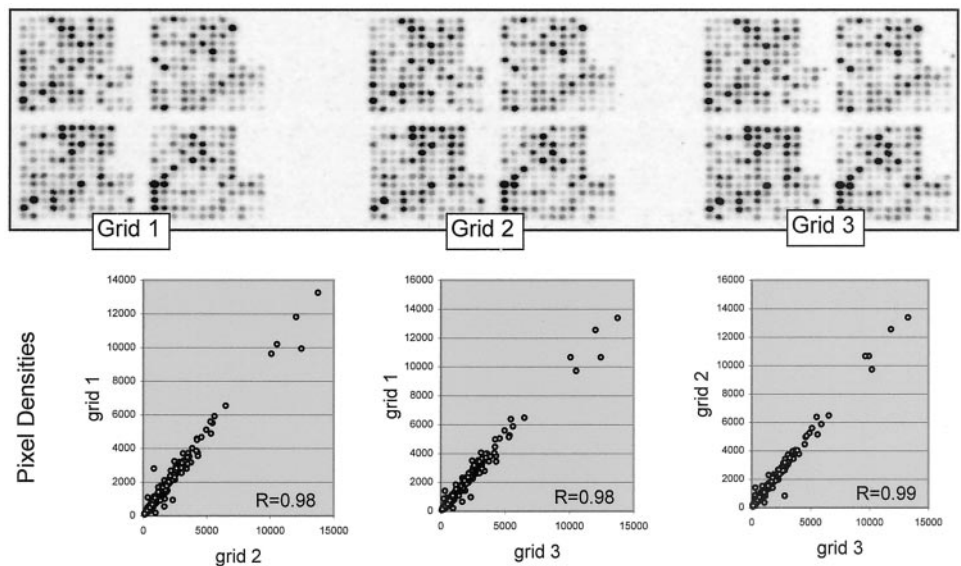
Analysis of Gene Expression Using the Ovachip. The genes arrayed on the Ovachip were chosen because of their importance in EOC according to our previous SAGE study (9). The complete list of the genes present on the Ovachip is available online.³ A typical hybridization of the Ovachip is shown in Fig. 1A. The entire set of 516 spots is present in triplicate on each membrane. The reproducibility within a membrane was remarkable as shown by the scatterplots and high level of correlation between the different replicates (Fig. 1B). The Ovachip was used to analyze a series of 11 stage III-IV ovarian tumors, 4 colon tumors, and various cell lines (Fig. 2). Visual inspection of the clustered data indicates that the ovarian tumors exhibit a distinct gene expression signature when analyzed with the Ovachip. This is evidenced by the presence of a highly correlated node containing all of the ovarian tumors. The ovarian cancer specimens are additionally subdivided into two main branches distinguished mostly by the behavior of a middle cluster of genes that appears to be highly

elevated in specimens ov11, ov8, ov2, and ov7 but not in the others. The colon tumors as well as the various cell lines cluster separately from the ovarian tumors and from each other, and exhibit quite heterogeneous gene expression patterns. The similarity between overall patterns of gene expression as measured with the Ovachip can be quantitated using P_{ov} . Fig. 3 shows the average P_{ov} values for all of the pair-wise comparisons of the specimens included in this study. It is apparent that when measured with the Ovachip the ovarian tumors are typically very similar to each other with an average P_{ov} between different ovarian tumors of 0.89 (Fig. 3). On the other hand, the ovarian specimens exhibited little similarity to colon tumors (average P_{ov} of only 0.11). Thus, the Ovachip is extremely sensitive at distinguishing colon from ovarian tumors. It is noteworthy that the average P_{ov} between the various colon cancers is only 0.73. It is important to emphasize that these correlation coefficients reflect gene expression as measured by the Ovachip and do not represent global gene expression. The fact that ovarian tumors appear more homogeneous than colorectal tumors is likely to be a consequence of our choice of ovarian-specific genes for the Ovachip. The similarity of gene expression signature of tumors (ovarian or colon) and the various cell lines is essentially nonexistent (P_{ov} close to 0), and the cell line expression patterns are unrelated to the tissue of origin (Fig. 3). This finding is similar to what we observed previously and suggests that cell lines represent a poor model for the study of tissue-specific gene expression (9). Cell lines exhibited some similarity to each other (average $P_{ov} = 0.64$) probably reflecting the similarities in culture conditions.

MDS has also been used to investigate gene expression relationships between different specimens (16, 17). Fig. 4 shows a MDS three-dimensional plot of all of the specimens included in this study. In this depiction of the data, the correlation coefficients are represented in a three-dimensional space, with samples exhibiting similar patterns of gene expression clustering closer together than samples with dissimilar patterns. Clearly, MDS was also extremely sensitive at differentiating ovarian tumors from colorectal tumors and cell lines.

Validation of the Ovachip. Although the global expression patterns obtained with this array were reproducible and consistent with our inclusion of ovarian-relevant genes, we wished to verify that individual gene expression measurements were accurate. Levels of expression for FR, SLPI, and IGFBP-2 were high in EOC as measured by the Ovachip (data not shown), which is consistent with our previous SAGE and RT-PCR results (10).

Fig. 1. Typical example of the results of a hybridization of an ovarian sample to the Ovachip. The 516 genes constituting the Ovachip are spotted in triplicate on a single membrane as described in "Materials and Methods." Scatter plots show a high level of reproducibility between the replicates with R values of 0.98 and 0.99.



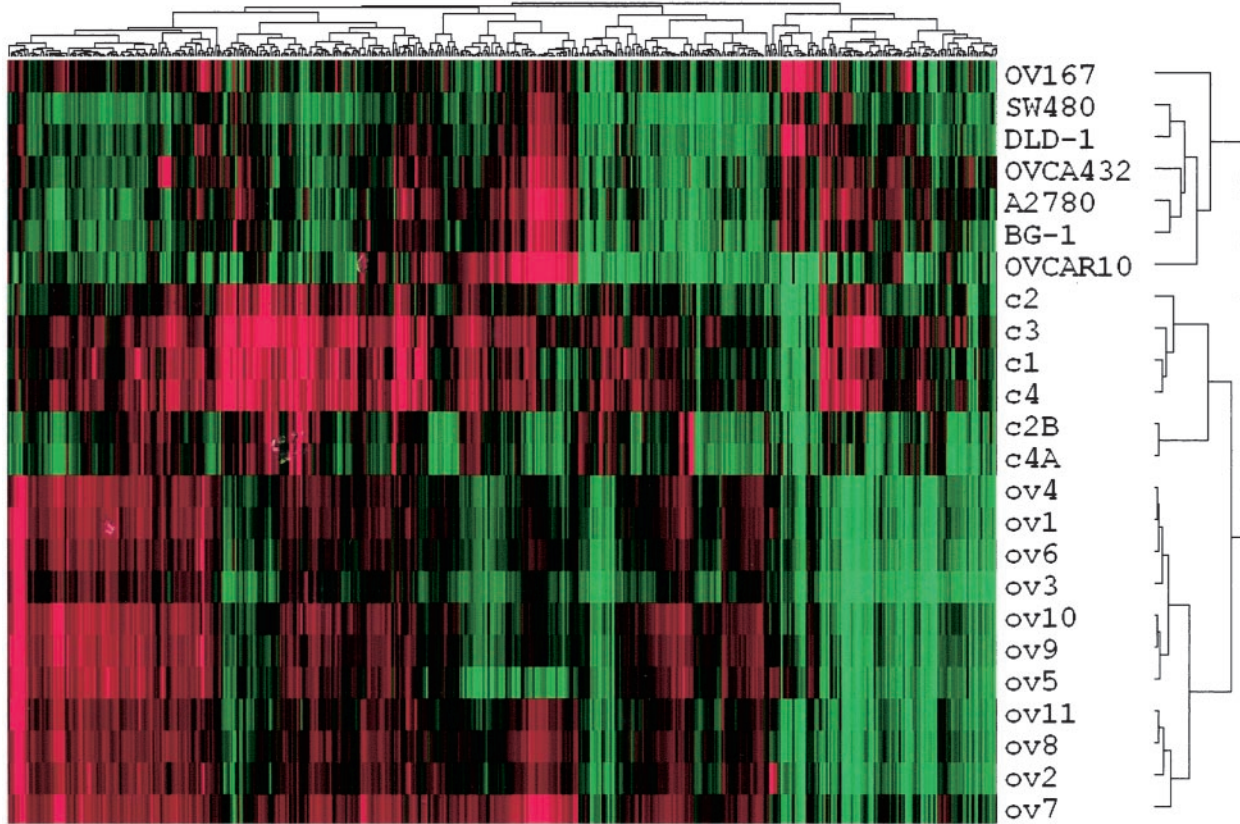


Fig. 2. Two-dimensional hierarchical clustering analysis applied to expression data from a set of 516 cDNAs measured in 7 cell lines, 11 ovarian tumors, and 6 colon tumors. The dendrogram represents gene expression patterns related to the tissue type (cell line, ovarian, and colon). Expression levels are relative to nonmalignant ovarian surface epithelial cells IOSE29EC and color-coded with red, green, and black corresponding to an increase, a decrease, and no change in gene expression, respectively. Ovarian tumor signature is obvious as all of the ovarian tumors cluster to a central node.

Typically, cDNA array data are validated by Northern or RT-PCR analysis of the genes demonstrating the most remarkable patterns of gene expression. For example, genes found to be highly up-regulated or down-regulated compared with a reference sample are often examined more closely using these techniques. Because we believe this may not be a completely fair validation of an array, we also wished to

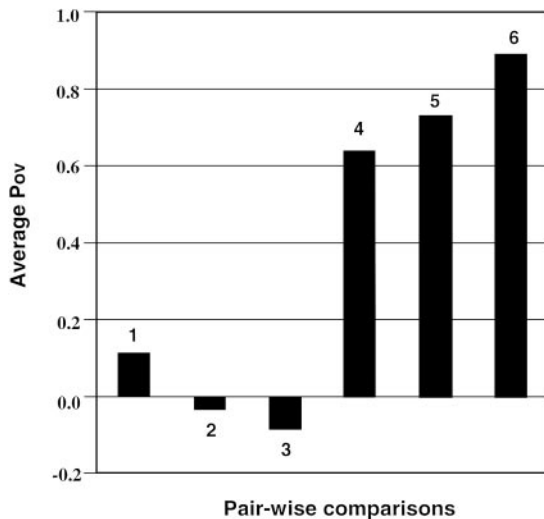


Fig. 3. Bar graph showing the P_{ov} for all pair-wise comparisons of the specimens included in this study. 1, ovarian tumors compared with colon tumors; 2, ovarian tumors compared with cell lines; 3, colon tumors compared with cell lines; 4, cell lines compared with each other; 5, colon tumors compared with each other; 6, ovarian tumors compared with each other.

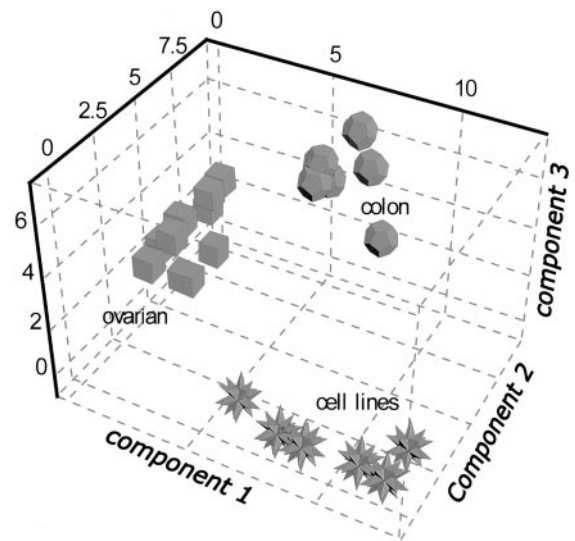


Fig. 4. MDS three-dimensional plot showing the clustering characteristics of all samples included in this study. Cell lines (stars), ovarian tumors (cubes), and colon tumors (spheres) are shown. The Ovachip is extremely sensitive at distinguishing ovarian tumors from other tissues.

examine genes with unremarkable expression patterns as measured by the Ovachip. We chose the genes *TAL-1*, *TCEB1*, *PMSA1*, and ApoE for their variety in Ovachip expression patterns. Fig. 5 compares the ability of the Ovachip and real-time RT-PCR to measure expression of these four genes in ovarian and colon tumors. It is clear that, whereas the results are not completely concordant, the general trend of gene

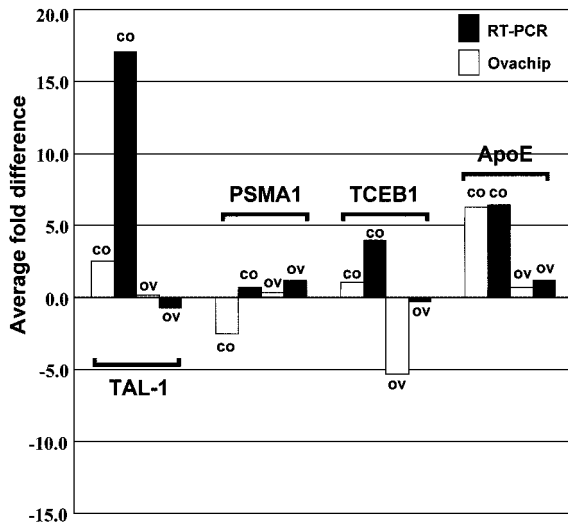


Fig. 5. Validation of individual genes expressed on the Ovachip using real-time RT-PCR. The graph shows the average fold difference (compared with normal ovarian surface epithelial cells) of the indicated genes as measured by real-time RT-PCR (■) or the Ovachip (□) in ovarian and colon tumors. The genes analyzed are TAL-1, TCEB1, PSMA1, and ApoE.

expression as measured by the array is generally verified by the highly accurate RT-PCR method. For example, both *TAL-1* and *TCEB1* are low in ovarian tumors and increased in colon tumors, with *TAL-1* higher than *TCEB1* in colon tumors. Similarly, ApoE is elevated both in colon and ovarian tumors, a trend observed with both techniques. These results prove the ability of the Ovachip to accurately measure levels of individual transcripts in cancer.

Identification of Differentially Expressed Genes. Using GeneSpring to analyze the hybridization data, 25 genes were found to be significantly up-regulated in ovarian cancer compared with nonmalignant ovarian surface epithelial cells, whereas 11 genes were found down-regulated (Table 1). A total of 26 genes were also up-regulated in colon cancer specimens, but only 1 gene was commonly elevated in ovarian and colon tumors. Of the 11 genes that were down-regulated in ovarian cancer, only 1 was also decreased in colon tumors (Table 1). Again, this is a likely consequence of our choice of genes relevant to ovarian tumorigenesis for inclusion on the Ovachip. Interestingly, *BRCA1* was found to be decreased using the Ovachip. *BRCA1* has been reported to be down-regulated at the mRNA level in the majority of sporadic ovarian cancers (18) by mechanisms that may involve promoter hypermethylation (19).

Coordinately Expressed Clusters of Genes. Many interesting clusters of genes with similar gene expression patterns can be identified from our study. Probably the most striking and interesting cluster was the IGF2 cluster, named after the gene with the highest level of up-regulation in ovarian cancer, IGF-II (Fig. 6). IGF-II is an imprinted gene expressed in the normal ovary and has been reported to be up-regulated in ovarian cancer, possibly through LOI (20, 21). The IGF2 cluster included 7 genes coordinately elevated in addition to IGF-II, including *TGF β -2*, a gene previously shown to be elevated in ovarian cancer (Ref. 22; Table 2). These genes may all be related to an important function in ovarian cancer development.

Another interesting cluster was composed of genes found to be coordinately down-regulated specifically in the ovarian carcinomas (Fig. 6). This cluster was named the CAK cluster because it included the *cdk7* as well as its regulatory subunit cyclin H (Fig. 6; Table 2). The CAK is a trimer consisting of *cdk7*, cyclin H, and *MAT1* (not on the Ovachip) and phosphorylates a conserved threonine residue on *cdks* that control cell cycle progression (23). The consequences of

down-regulation of this activity are unclear but would clearly affect cell cycle control and possibly response to DNA damage and genomic integrity. The CAK cluster comprises a total of 10 genes, including the *FGR* oncogenes, the selenium binding protein 1 and filamin A (Table 2).

DISCUSSION

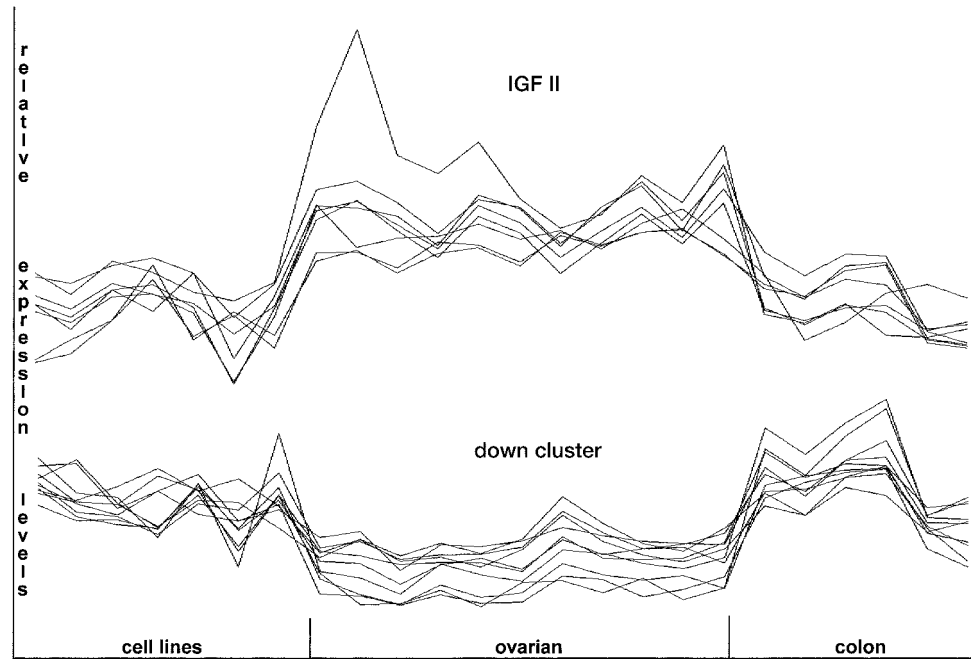
Ovarian cancer is a poorly understood disease at the molecular level. Despite a recent series of exciting advances in the field leading to a better characterization of ovarian-specific gene expression signatures and potential new tumor suppressor genes, the molecular pathways crucial for initiation and progression of EOC remain mostly unknown. In fact, the exact nature of the tissue of origin is still a matter of debate. Although EOC is generally thought to arise from the layer of mesothelial cells covering the ovaries, a convincing argument can be made that the actual precursor is a different tissue altogether, namely the secondary Mullerian system (22). Clearly, the elucidation of these puzzling questions will require coordinated efforts as well as novel tools and reagents. In this report, we have constructed a specialized cDNA array for the study of EOC. Although our previous SAGE study of ovarian malignancy revealed major gene expression patterns and many differentially expressed genes (9), SAGE does not allow high throughput analysis of many tumors, which may be required to identify relevant pathways. A small, focused array has several advantages compared with the large arrays currently widely used for gene expression analysis. First, a small, specialized chip includes only genes relevant to the biological process of interest, eliminating noise and allowing the identification of relationships that may otherwise be lost (11, 23). Secondly, it allows a larger level of

Table 1 Genes differentially expressed in ovarian tumors as measured by the Ovachip

Genes	Accession
Up-regulated genes	
Insulin-like growth factor II (<i>IGF2</i>)	NM_000612
PTP receptor type (<i>PTPRC</i>)	XM_016748
Fms-related tyrosine kinase 1 (<i>FLT1</i>)	XM_039993
Heat-shock protein 90 kd α (<i>HSP90</i>)	NM_074225
Cyclin-dependent kinase 6 (<i>CDK6</i>)	NM_001259
Checkpoint suppressor 1 (<i>CHES1</i>)	XM_007389
RAB1, member RAS oncogene family (<i>RAB1</i>)	XM_046674
Cisplatin resistance-associated protein (<i>CRA</i>)	XM_051918
Nidogen (Enactin) (<i>NID</i>)	XM_002042
Orphan G protein-coupled receptor (<i>RDC1</i>)	U67784
Ras inhibitor (<i>RIN1</i>)	NM_004292
Transformation growth factor β 2 (<i>TGFβ2</i>)	XM_001754
Laminin α 3 nicein (<i>LAMA</i>)	NM_000227
Carboxylesterase 2 (<i>CES2</i>)	NM_003869
Membrane metallo-endopeptidase (<i>MME</i>)	XM_030171
H4 (D10S170) Transforming sequence	XM_005753
MutS Homolog 3 (<i>MSH3</i>)	XM_003992
EST, similar to mu-type opioid receptor	R31984
Butyrate response factor 1 (<i>BRF1</i>) ^a	NM_001519
EST	R10292
Throboxane A synthase 1 (<i>TBXAS1</i>)	NM_030984
Nuclear factor I χ (<i>NFIX</i>)	XM_057080
E2F transcription factor 5 (<i>E2F5</i>)	NM_001951
Fc- γ receptor IIIa (<i>CD16</i>)	NM_000569
Small proline rich protein 1 (<i>SPRR1B</i>)	XM_096133
Down-regulated genes	
Forkhead box (<i>FOXF1</i>)	XM_008078
Ribosomal protein L7a (<i>RPL7A</i>)	BC021979
Basic transcription factor 3 (<i>BTF3</i>)	NM_001202
Mitogen-activated protein kinase 1 (<i>MAPK1</i>)	XM_036967
Lactate dehydrogenase A (<i>LDHA</i>)	NM_005566
β -tubulin (<i>TUBB</i>) ^a	AF070561
Breast Cancer 1, early onset (<i>BRCA1</i>)	AF005068
Nucleophosmin (<i>NPM1</i>)	BC021983
Threonyl tRNA synthase (<i>TARS</i>)	NM_064096
Decay accelerating factor (<i>DAF/CD55</i>)	XM_055716
Myosin light chain kinase (<i>MYLK</i>)	XM_042186

^a Up-regulated or down-regulated in colon tumors as well.

Fig. 6. Genespring analysis depicting gene coregulation in the IGF2 cluster and in the CAK cluster. Tissue type (cell lines, ovarian tumors, and colon tumors) is shown on the abscissa, and relative gene expression levels are plotted on the ordinate. Nonmalignant ovarian surface epithelial cells IOSE29EC are used as control.



replication for the same RNA input. For example, the Ovachip is entirely contained in triplicate on a single membrane (see Fig. 1) allowing three independent measurements from a single hybridization and increasing statistical power (13). Finally, the small chip greatly simplifies data analysis, and reduces time and computer power required to obtain expression information in final form. Again, all of these advantages are the results of the exclusion of genes that are not involved in the process under study. The construction of focused array requires previous knowledge of gene expression profiles for the tissue of interest. Considering the expanding number and size of public and commercial gene expression databases, this problem should not represent a major hurdle.

All of the ovarian tumors have similar Ovachip signatures, which are clearly different from the signatures obtained with colon tumors (Fig. 2). This is likely the result of our selection of genes relevant to EOC for selective inclusion on the array. This suggests that this array would be extremely sensitive at identifying EOC when histopathological parameters may be ambiguous. Because hybridization can be performed with small amounts of starting RNA, the Ovachip could be

used to distinguish ambiguous clinical specimens. It is also possible that small variations of this known pattern of gene expression may have relevant biological significance. For example, we have found that a low-malignant potential ovarian tumor exhibits a significantly different Ovachip signature compared with the typical serous ovarian carcinomas (data not shown). Thus, the Ovachip may be useful in identifying small but significant gene expression differences that are relevant to the clinical behavior of these tumors such as growth and invasive capabilities. In this context, it is also clear that the Ovachip may be used advantageously in ovarian cancer research. Indeed, as described above, this array may allow the identification of subtle differences that larger arrays may miss because of the presence of many irrelevant genes that increase the noise during data analysis (11). In our hands, small arrays have provided more accurate and reproducible gene expression data, which could be validated using real-time RT-PCR (Fig. 5). The genes that exhibit altered expression levels in ovarian cancer (Table 1) may all represent targets for diagnosis or mechanism-based therapy.

Using the Ovachip, we have found many genes differentially expressed in ovarian cancer (Table 1), including two major clusters of coordinately regulated genes that may be important in ovarian cancer (Fig. 6; Table 2). The IGF2 cluster includes seven genes apparently functionally unrelated. Relaxation of IGF2 LOI has been suggested to be at least partly responsible for its abnormal expression in ovarian cancer, and it will be interesting to see whether the other genes of the IGF2 cluster also exhibit abnormal methylation patterns of their promoters. It is intriguing that this cluster includes the CRA and several genes involved in cell cycle control. The IGF2 expression signature may be related to the modulation of cell cycle checkpoints and acquisition of drug resistance. In addition, this cluster includes *FLT1*, one of the VEGF receptors (26). *FLT1* expression has been reported in tumor cells, endothelial cells, and stromal fibroblasts of various tumors and may be part of an important autocrine loop (27). Considering the importance of angiogenesis to ascites development and ovarian cancer metastasis, the identification of *FLT1* as part of this clusters suggests that these genes may be related to advanced disease.

A cluster of highly coordinately expressed down-regulated genes

Table 2 Members of the IGF2 and CAK clusters

Cluster	Accession
IGF2 cluster	
Insulin-like growth factor II (<i>IGF2</i>)	NM_000612
Checkpoint suppressor 1 (<i>CHES1</i>)	XM_007389
Cisplatin resistance-associated protein (<i>CRA</i>)	XM_051918
Cyclin-dependent kinase 6 (<i>CDK6</i>)	NM_001259
PTP receptor type (<i>PTPRC</i>)	XM_016748
Transforming growth factor 2 (<i>TGFB2</i>)	XM_001754
Protein tyrosine kinase-7 (<i>PTK7</i>)	AF447176
EST	R10292
CAK cluster	
AXL receptor tyrosine (<i>AXL</i>)	XM_015505
Cyclin H (<i>CCNH1</i>)	AF477979
S100 calcium binding protein A2 (<i>S100A2</i>)	NM_005978
v-fgr oncogene homolog (<i>FGR</i>)	XM_001640
MAPKKK 8 (<i>MAP3K8</i>)	XM_030523
Selenium binding protein 1 (<i>SELENBP1</i>)	NM_003944
Cyclin-dependent kinase 7 (<i>CDK7</i>)	XM_010834
Cytochrome c-1 (<i>CYC1</i>)	NM_0001916
EST	AA962294
Filamin A, α (<i>FLNA</i>)	XM_048404

was also identified (Fig. 6). The main feature of this cluster is the presence of *cdk7* and its regulatory subunit cyclin H, comprising two of the three necessary components that make up the CAK. The third component of this complex, MAT1 [also known as CAK assembly factor and MNAT1 (23)], was not present on our array. It is unclear why these genes would be down-regulated in ovarian cancer as they have previously been found to be moderately up-regulated in other cancers (28, 29). Changes in expression of these genes would clearly affect cell cycle control and progression and may influence important checkpoints in ovarian cancer. We are currently investigating genes from both the IGF2 cluster and the CAK cluster for their role in ovarian tumorigenesis.

In summary, we have constructed and tested a specialized ovarian cancer chip that we named the Ovachip. The advantages of this small, specialized array are numerous and enabled us to identify novel clusters of genes differentially expressed in ovarian cancer. It is our hope that the Ovachip will facilitate progress in understanding the etiology of this disease and in its clinical management.

ACKNOWLEDGMENTS

We thank Drs. Ellen Pizer, Leticia Rangel, Rachana Agarwal, and Ashani Weeraratna, for helpful comments on the manuscript.

REFERENCES

- Rustin, G. J., van der Burg, M. E., and Berek, J. S. Advanced ovarian cancer. Tumor markers. *Ann. Oncol.*, *4*: 71–77, 1993.
- Ozols, R. F., and Young, R. C. Chemotherapy of ovarian cancer. *Semin. Oncol.*, *11*: 251–263, 1984.
- Sasano, H., Garrett, C. T., Wilkinson, D. S., Silverberg, S., Comerford, J., and Hyde, J. Protooncogene amplification and tumor ploidy in human ovarian neoplasms. *Hum. Pathol.*, *21*: 382–391, 1990.
- Matias-Guiu, X., and Prat, J. Molecular pathology of ovarian carcinomas. *Virchows Arch.*, *433*: 103–111, 1998.
- Cliby, W., Ritland, S., Hartmann, L., Dodson, M., Halling, K. C., Keeney, G., Podratz, K. C., and Jenkins, R. B. Human epithelial ovarian cancer allelotyping. *Cancer Res.*, *53*: 2393–2398, 1993.
- Schummer, M., Ng, V. L. V., Baumgarner, R. E., Nelson, P. S., Schummer, B., Bednarski, D. W., Hassell, L., Baldwin, R. L., Karlan, B. Y., and Hood, L. Comparative hybridization of an array of 21 500 ovarian cDNAs for the discovery of genes overexpressed in ovarian carcinomas. *Gene*, *238*: 375–385, 1999.
- Welsh, J. B., Zarrinkar, P. P., Sapinoso, L. M., Kern, S. G., Behling, C. A., Monk, B. J., Lockhart, D. J., Burger, R. A., and Hampton, G. M. Analysis of gene expression profiles in normal and neoplastic ovarian tissue samples identifies candidate molecular markers of epithelial ovarian cancer. *Proc. Natl. Acad. Sci. USA*, *98*: 1176–1181, 2001.
- Shridhar, V., Lee, J., Pandita, A., Iturria, S., Avula, R., Staub, J., Morrissey, M., Calhoun, E., Sen, A., Kalli, K., Keeney, G., Roche, P., Cliby, W., Lu, K., Schmandt, R., Mills, G. B., Bast, R. C., Jr., James, C. D., Couch, F. J., Hartmann, L. C., Lillie, J., and Smith, D. I. Genetic analysis of early- versus late-stage ovarian tumors. *Cancer Res.*, *61*: 5895–5904, 2001.
- Hough, C. D., Sherman-Baust, C. A., Pizer, E. S., Montz, F. J., Im, D. D., Rosenshein, N. B., Cho, K. R., Riggins, G. J., and Morin, P. J. Large-scale serial analysis of gene expression reveals genes differentially expressed in ovarian cancer. *Cancer Res.*, *60*: 6281–6287, 2000.
- Hough, C. D., Cho, K. R., Zonderman, A. B., Schwartz, D. R., and Morin, P. J. Coordinately up-regulated genes in ovarian cancer. *Cancer Res.*, *61*: 3869–3876, 2001.
- Getz, G., Levine, E., and Domany, E. Coupled two-way clustering analysis of gene microarray data. *Proc. Natl. Acad. Sci. USA*, *97*: 12079–12084, 2000.
- Auersperg, N., Pan, J., Grove, B. D., Peterson, T., Fisher, J., Maines-Bandiera, S., Somasiri, A., and Roskelley, C. D. E-cadherin induces mesenchymal-to-epithelial transition in human ovarian surface epithelium. *Proc. Natl. Acad. Sci. USA*, *96*: 6249–6254, 1999.
- Tanaka, T. S., Jaradat, S. A., Lim, M. K., Kargul, G. J., Wang, X., Grahovac, M. J., Pantano, S., Sano, Y., Piao, Y., Nagaraja, R., Doi, H., Wood, W. H., III, Becker, K. G., and Ko, M. S. Genome-wide expression profiling of mid-gestation placenta and embryo using a 15,000 mouse developmental cDNA microarray. *Proc. Natl. Acad. Sci. USA*, *97*: 9127–9132, 2000.
- Eisen, M. B., Spellman, P. T., Brown, P. O., and Botstein, D. Cluster analysis and display of genome-wide expression patterns. *Proc. Natl. Acad. Sci. USA*, *95*: 14863–14868, 1998.
- Simon, R., Desper, R., Papadimitriou, C. H., Peng, A., Alberts, D. S., Taetle, R., Trent, J. M., and Schaffer, A. A. Chromosome abnormalities in ovarian adenocarcinoma: III. Using breakpoint data to infer and test mathematical models for oncogenesis. *Genes Chromosomes Cancer*, *28*: 106–120, 2000.
- Bittner, M., Meltzer, P., Chen, Y., Jiang, Y., Seftor, E., Hendrix, M., Radmacher, M., Simon, R., Yakhini, Z., Ben-Dor, A., Sampas, N., Dougherty, E., Wang, E., Marincola, F., Gooden, C., Lueders, J., Glatfelter, A., Pollock, P., Carpten, J., Gillanders, E., Leja, D., Dietrich, K., Beaudry, C., Berens, M., Alberts, D., and Sondak, V. Molecular classification of cutaneous malignant melanoma by gene expression profiling. *Nature (Lond.)*, *406*: 536–540, 2000.
- Hedenfalk, I., Duggan, D., Chen, Y., Radmacher, M., Bittner, M., Simon, R., Meltzer, P., Gusterson, B., Esteller, M., Kallioniemi, O. P., Wilfond, B., Borg, A., and Trent, J. Gene-expression profiles in hereditary breast cancer. *N. Engl. J. Med.*, *344*: 539–548, 2001.
- Russell, P. A., Pharoah, P. D., De Foy, K., Ramus, S. J., Symmonds, I., Wilson, A., Scott, I., Ponder, B. A., and Gayther, S. A. Frequent loss of BRCA1 mRNA and protein expression in sporadic ovarian cancers. *Int. J. Cancer*, *87*: 317–321, 2000.
- Baldwin, R. L., Nemeth, E., Tran, H., Shvartsman, H., Cass, I., Narod, S., and Karlan, B. Y. BRCA1 promoter region hypermethylation in ovarian carcinoma: a population-based study. *Cancer Res.*, *60*: 5329–5333, 2000.
- Chen, C. L., Ip, S. M., Cheng, D., Wong, L. C., and Ngan, H. Y. Loss of imprinting of the insulin-like growth factor II and H19 genes in epithelial ovarian cancer. *Clin. Cancer Res.*, *6*: 474–479, 2000.
- Kim, H. T., Choi, B. H., Niikawa, N., Lee, T. S., and Chang, S. I. Frequent loss of imprinting of the H19 and IGF-II genes in ovarian tumors. *Am. J. Med. Genet.*, *80*: 391–395, 1998.
- Bartlett, J. M., Langdon, S. P., Scott, W. N., Love, S. B., Miller, E. P., Katsaros, D., Smyth, J. F., and Miller, W. R. Transforming growth factor β isoform expression in human ovarian tumours. *Eur. J. Cancer*, *33*: 2397–2403, 1997.
- Kaldis, P., and Solomon, M. J. Analysis of CAK activities from human cells. *Eur. J. Biochem.*, *267*: 4213–4221, 2000.
- Dubeau, L. The cell of origin of ovarian epithelial tumors and the ovarian surface epithelium dogma: does the emperor have no clothes? *Gynecol. Oncol.*, *72*: 437–442, 1999.
- West, M., Blanchette, C., Dressman, H., Huang, E., Ishida, S., Spang, R., Zuzan, H., Olson, J. A., Jr., Marks, J. R., and Nevins, J. R. Predicting the clinical status of human breast cancer by using gene expression profiles. *Proc. Natl. Acad. Sci. USA*, *98*: 11462–11467, 2001.
- Kaipainen, A., Korhonen, J., Pajusola, K., Aprelikova, O., Persico, M. G., Terman, B. I., and Alitalo, K. The related FLT4, FLT1, and KDR receptor tyrosine kinases show distinct expression patterns in human fetal endothelial cells. *J. Exp. Med.*, *178*: 2077–2088, 1993.
- Dias, S., Hattori, K., Heissig, B., Zhu, Z., Wu, Y., Witte, L., Hicklin, D. J., Tatenos, M., Bohlen, P., Moore, M. A., and Rafii, S. Inhibition of both paracrine and autocrine VEGF/VEGFR-2 signaling pathways is essential to induce long-term remission of xenotransplanted human leukemias. *Proc. Natl. Acad. Sci. USA*, *98*: 10857–10862, 2001.
- Bartkova, J., Zemanova, M., and Bartek, J. Expression of CDK7/CAK in normal and tumor cells of diverse histogenesis, cell-cycle position and differentiation. *Int. J. Cancer*, *66*: 732–737, 1996.
- Mouriaux, F., Casagrande, F., Pillaire, M. J., Manenti, S., Malecaze, F., and Darbon, J. M. Differential expression of G1 cyclins and cyclin-dependent kinase inhibitors in normal and transformed melanocytes. *Investig. Ophthalmol. Vis. Sci.*, *39*: 876–884, 1998.